AIAA 89-1798
Study of Plane Underexpanded Air Jets in Water

E. Loth
Naval Research Laboratory
Washington, DC
G. Faeth
University of Michigan
Ann Arbor, MI

AIAA 20th Fluid Dynamics, Plasma Dynamics and Lasers Conference
Buffalo, New York / June 12–14, 1989

STUDY OF PLANE UNDEREXPANDED AIR JETS IN WATER

Eric Loth* , Gerard M. Faeth**

University of Michigan, Aerospace Engineering, Ann Arbor, MI 48109

Abstract

An experimental and theoretical investigation of the structure of plane underexpanded air jets in water was conducted. To characterize the structure and mixing properties of these jets, the following measurements were made: void fraction profiles, static pressure distributions, and entrainment rates. Test conditions varied from adapted sonic jets to sonic underexpanded flow with underexpansion ratios (exit to ambient static pressure) as high as four. Flow visualization was also used to investigate jet boundaries, dynamics of discharge, and compressible wave fields. A locally-homogeneous flow model (implying negligible velocity and temperature differences between the phases) was developed, with the external expansion represented by a simple equivalent adapted jet exit condition.

Static pressure measurements confirmed the presence of a shock-wave-containing external-expansion region for underexpanded air jets in water, similar to results observed for underexpanded air jets in air. The void fraction profiles were two to three times wider than single-phase jet scalar widths. This is a result of the strong sensitivity of void fraction to mixing levels caused by the large density ratio of the phases. Predictions of void fraction profiles, jet half-widths and mass entrainment were encouraging, but performance was found to be sensitive to initial conditions and effects of large-scale unsteadiness.

Introduction

The objective of this investigation is to understand the multiphase flow mixing resulting from the injection of an underexpanded jet of air into a quiescent water bath. There are several direct applications of gas injection into liquids, including: direct-contact condensers, gas dissolution systems, reservoir destratification systems and stored chemical energy propulsion systems (SCEPS). Such systems require high underexpansion ratios to insure stable operation; therefore, understanding the multiphase flow properties as they interact with the supersonic wave structure is crucial. Typically, an air jet core is maintained for some distance downstream of the passage exit until finally turbulent mixing and entrainment prevail, resulting in a constant pressure bubbly flow with the associated buoyancy effects. An important aspect of such injection is the characteristic unsteadiness due to the complex momentum transfer of the flow. This is quite evident for subsonic jets, but has also been observed to a lesser degree for adapted and underexpanded sonic jets by Cho et al.[1], Lin[2], and Surin et al.[3].

Earlier studies of gas jets in liquids such as Kerney et al.[4], Chen and Faeth[5], and Avery and Faeth[6] were confined to gross parameters such as penetration distances and liquid temperature profiles. Analysis typically consisted of integral entrainment models based on the locally homogeneous flow approximation (LHF) with reasonable success for both reacting and condensing integral turbulent jet properties. The work by Tross[7] is perhaps the study most closely related to the present work since it included intrusive measurements of void fraction (volume fraction of gas to total volume) and dynamic pressure profiles for a round underexpanded turbulent air jet in a quiescent water bath. The considerable uncertainty in existing probe measurements, due to the large density difference and the effects of surface tension on the probes, indicates the need for extensive non-intrusive measurements of void fraction, liquid entrainment velocities and visualization of the compressible wave field for underexpanded gas injection into liquids.

---

*currently Aerospace Engineer, Laboratory for Computational Physics and Fluid Dynamics, Naval Research Laboratory, Washington D. C., Member AIAA.

**Modine Professor of Aerospace Engineering, Fellow AIAA.

Experimental Methods

The test apparatus included a water-filled tank (2 m in length, 2 m in height, 1 m in width), a traversable injector and glass walls to allow flow visualization with high-speed, flash and shadowgraph photography. Instrumentation was also employed to allow static pressure measurements with a probe; non-intrusive measurements of void fractions with a gamma-ray absorption system; and velocity measurements with a laser-Doppler anemometry (LDA) system. A schematic of the injector is shown in Figure 1. The injector was directed vertically upward and was mounted on a support brace which could be traversed in the horizontal and vertical directions to within 0.1 mm and 1 mm, respectively. Thus the axial and lateral distributions of the multiphase jet were obtained while keeping the instrumentation stationary.

The plane (two-dimensional) brass injector consisted of a brass plenum chamber feeding into a 6:1 lateral contraction, designed to provide a uniform exit velocity across the exit width, b, of 4.8 mm, which yielded an exit aspect ratio of eleven. Glass sidewalls provided optical access for an axial distance of 13 exit widths and a total lateral distance of 16 exit widths. The air supply was drawn from high pressure tanks (filtered and dried to a dew point less than 240 K) and was monitored for mass flow and stagnation temperatures.

Flash photographs of 1 ms exposure were used to observe mixing region growth; high-speed motion pictures (1 frame/ms) were used to study flow unsteadiness, and flash shadowgraphs of 1 ms exposure were used to document the compressible wave field in the air core. This compressible wave field was also measured via a 1 mm static pressure tap placed along the axis centerline of the jet (in place for this diagnostic only) which was fixed far upstream and downstream of the nozzle exit. The stainless steel pressure tap is similar to the probe used by Eggers[8] and was equipped with a slight air pressure supply to purge any excess water in the system. In addition, a fast-response hydrophone (± 2 db for 1 kHz to 40 kHz) was used to detect the presence of acoustic resonance.

A gamma-ray absorption technique was used to measure void fractions since it is a well established non-intrusive technique, see Ohba[9]. Since the attenuation of a gamma-ray beam depends chiefly on the amount of liquid penetrated by its path, measurements normal to a two-dimensional jet will yield pointwise variation of void fraction based on calibrated intensities. A 10 mCi concentration of Cobalt-57 was chosen as the gamma beam source since it has an extended half-life, a nearly 100% decay scheme, and a photon energy level which corresponds to a desirable attenuation range for the typical water lengths encountered. The highly collimated gamma beam of 122 and 136 keV was detected with a NaI crystal and the signal was processed with spectroscopic grade equipment (see Figure 2). The traversing and timer/counter device were linked through an IBM AT to provide completely automated testing throughout a lateral survey. Maximum experimental uncertainties of void fraction are estimated to be less than 9%, and less than 5% for dynamic bias.

Mean and fluctuating velocities for the liquid entrainment and gas jet initial conditions were measured with a single-channel frequency-shifted LDA arrangement. Off axis detection resulted in a 700 μm diameter probe volume diameter for the exit gas velocity and a 260 μm diameter for the entrainment velocity measurements. Gas exit velocity uncertainties were estimated to be 5% and 25% for mean and fluctuating quantities respectively. Defining the entrainment rate, $d\dot{m}/dx$, as the rate of increase of mass flux of the jet with streamwise distance per unit longitudinal length, one may form a dimensionless entrainment coefficient from scaling laws:

$$C_e = d\dot{m}/dx \,/\, (F_e\, r_\infty\, b)^{1/2} \qquad (1)$$

where F_e is the jet exit force per unit longitudinal length. Estimated experimental uncertainties were less than 10% for the dimensionless entrainment coefficient.

The sonic exit conditions produced Reynolds numbers typically 10^5-10^6 and Richardson's number of typically 10^{-4}; thus inertial forces are expected to dominate the flow near the injector (for further apparatus details, see Loth[10]).

Numerical Methods

Analysis was similar to the approach proposed by Chen and Faeth[5] to treat flows of this type. The method has been evaluated using structure measurements for a wide range of multiphase jets studuied in this laboratory (see Faeth[11]). The objective of present work was to extend this evaluation to underexpanded gas jets in liquids. This formulation appears in Loth[10] and Facth[11] and will only be briefly described.

The three major assumptions of the analysis are as follows: (1) use of the locally-homogeneous flow (LHF) approximation to treat multiphase flow effects; (2) use of the equivalent exit condition (EEC) to treat the external expansion region of the underexpanded jets; (3) use of a second order turbulence model to treat mixing. The LHF approximation implies negligible relative velocities between phases and local thermodynamic equilibrium. Therefore, the flow is treated like a single-phase fluid having large density variations due to changes in gas concentration while separated flow parameters, such as drop and bubble size distributions, do not enter the formulation. Recent evaluations of the LHF approximation suggest reasonably good performance in the near injector region of sprays and bubbly jets (Faeth[11]; Ruff et al.[12]; and Sun and Faeth[13]); it therefore seems prudent to to evaluate the performance of the LHF approximation before undertaking the additional complications of separated flow analysis.

The equivalent exit conditions (EEC) approximation is frequently used to avoid the complexities of treating gas-dynamic phenomena in external expansion regions when estimating turbulent mixing for both single- and multi-phase flows (Avery and Faeth[6], Cheuch et al.[14], Kerney et al.[4]). This approximation assumes that the external expansion process can be represented with jet exit conditions (width, velocity, etc...) based on an isentropic expansion of the nozzle flow to ambient pressure. This approach has been effective for estimating the mixing properties of gas injection into gases as shown by Cheuch et al.[14] and conserves mass, momentum and energy for the flow. Clearly, it is of interest to evaluate the performance of the EEC approximation for the present study.

Due to the high Reynolds numbers of the present flows, some degree of modeling must be accepted to treat the mixing properties. The description and use of a k-ε-g turbulence model model with the conserved scalar formalism for low-speed two-phase flows was proposed by Chen and Faeth[9] but is extended here to include mass-weighted (Favre-) averages instead of time-averages, in order to eliminate numerous density fluctuation terms, as recommended by Bilger[15]. The formulation involves solving governing equations for conservation of mass, axial momentum, mean mixture fraction, turbulence kinetic energy, the rate of dissipation of kinetic energy, and mixture fraction fluctuations squared. The exit flow was initiated as uniform across the exit in all quantities with the same turbulence constants used for previous two-dimensional single-phase studies (Lai, et al.[16]). The details of the formulation are described in Loth[10] and Faeth[11] and has been shown to provide reasonable pointwise distributions for several flows (Chen and Faeth[5], Faeth,[11], Ruff et al.[12], Sun and Faeth[13], Loth and Faeth[17]). Since present measurements suggested enhanced mixing very close to the injector, a slightly mixed profile of mixture fraction was used in addition to the standard initial conditions of uniform flow. This was prescribed by a sinusoidal variation of void fraction across the equivalent jet width, b_{eq}, as shown in Figure 3.

Other major assumptions for the model include steady (in the mean) two-dimensional flow; equal exchange coefficients of all species, phases and heat; buoyancy only considered in the governing equations of the mean (vs. turbulent) quantities; the ideal-gas approximation; the boundary-layer approximation; and the assumption of constant specific heats for both phases. For single-phase shear flows, these assumptions have been shown to provide good predictions of mean and fluctuating quantities for several types of flows mentioned above including studies by Lai, et al.[16] for plane jets. Results reported in the following used 360 cross-stream grid nodes, with streamwise increments chosen to be less than 0.2% of the current flow width and node doubling resulting in less than 1 percent change of predictions.

Results and Discussion

Flow Definition

Flash photographs reveal a clearly irregular jet edge, presumably to the high turbulence levels of the jet itself; a typical photograph is shown in Figure 4A for an underexpansion ratio, $\dot{m}/\dot{m}_s$, of three. The oval-shaped air core just past the exit plane is the first oblique shock cell of the external expansion region. Downstream of this cell, the jet core does not appear to significantly expand again and large amounts of droplets are entrained into the gas region. Higher underexpansion ratios (exit to ambient static pressure) yield finer asperities of the visible gas surface: this may be attributed to the decreasing turbulence length scales as the Reynolds number of the flow is increased. The observed rapid radial growth of the flow can be attributed to the extreme sensitivity of void fraction to low levels of mixture fraction. The increased angle near the injector exit at the larger underexpansion ratios can be attributed to the

presence of the external expansion region field near the exit.

Large scale unsteadiness was noted for the multiphase flow field which tended to decrease in intensity and frequency as the level of underexpansion increased; these disturbances appear to originate at the point of injection. The high-speed motion pictures gave further evidence of the rapid radial growth of the flow, as well as the unsteadiness which was found to be an innate part of air injection into water at the underexpansion levels considered in this study. This is similar to results obtained for round jets by Loth and Faeth[17], Cho et al.[1], and Surin et al.[3].

Shadowgraph photography was employed for the plane jets at all test conditions considered during this investigation. For air injected into still air, the photographs were similar to those taken by Sheeran and Dosanjh[18] in terms of shock-cell width and length; a typical photograph is shown for an underexpansion ratio of three in Figure 4B. Near the exit, the presence of expansion fans can be detected. These fans reflect off the constant pressure boundary to form compression waves, which coalesce to form the observed oblique shock waves. The intercepting shocks cross at the end of the shock-cell and a second shock-cell appears; this process repeats for up to five shock-cells depending on the underexpansion ratio.

Shadowgraphs were also obtained for the injection of air into still water. The presence of the four plate glass walls and the liquid degraded the quality of these photographs, but qualitative characteristics could still be observed. Figure 4C shows a typical shadowgraph for an underexpansion ratio of three. Close observation of such photographs showed the presence of initial expansion fans and compression waves within the jet core, similar to air injection into air. This provides visual evidence that the external expansion region exists for gas injection into liquids. The rapid erosion of the second shock cell, seen in the flash photographs, can also be observed.

Velocity measurements at the passage exit were obtained with the air injection into still air, to remove any of the effects of gas-liquid unsteadiness. The plane converging nozzle was designed to yield a uniform exit velocity profile. The measured mean velocity profile is reasonably uniform except for the last 10% near the jet edge. The variation is probably due to gradient broadening of the LDA measurements, since the measuring volume is roughly equal to one-tenth of the radius. Fluctuating velocities indicate a turbulence level of roughly three percent uniformly across the exit; as stated above, the resolution is not sufficient to resolve the boundary layer. From these measurements, the nozzle appears to provide a uniform exit velocity with relatively low turbulence intensities.

Another important feature of the passage exit condition is the presence of acoustic feedback within the shock-cell pattern. Acoustic feedback arises as a result of pressure disturbances traveling upstream near the edge of the jet, reflecting from the surfaces near the exit plane of the nozzle and resonating at a particular frequency. The tuning condition is set by the sound wave speed of the ambient fluid and an acoustic reflection distance from the jet exit to some downstream position of the external expansion region, associated with one of the shock cells. Sherman et al.[19] and Glass[20] have reported substantially increased mixing due to acoustic feedback for underexpanded air jets in air, with dominant feedback frequencies approximately proportional to the sonic speed divided by the first or second shock-cell length.

Measurements with a hydrophone at a lateral position of six exit widths from the centerline and six exit widths downstream were completed for the 4.8 mm plane injector, for air injected both into air and into water. Power spectral densities of the acoustic signal are plotted as a function of frequency in Figure 5. Measurements were made for frequencies of up to 62 kHz (the approximate Strouhal number), with significant signal content found in the 1-25 kHz regime. There is substantial evidence of acoustic feedback in Figure 4.11 for all the underexpansion ratios for the plane air jet into air. Feedback peaks are especially large at underexpansion ratios of two and three, with frequencies corresponding to acoustic reflection distances of several exit widths. The flat surface along the exit plane is probably responsible for this dramatic increase in acoustic feedback, since it provides a reflecting surface for acoustic disturbances. However, injection into water yields lower acoustic levels at the high frequencies, ca. 5-25 kHz, and no evidence of acoustic feedback despite the reflective surface. This may be attributed to the effects of widely varying acoustic velocities in the multiphase flow; in addition, the presence of bubbles in the multiphase flow has been found to damp pressure waves, as reported by Borisov[21].

Flow Structure

Time-averaged static pressure measurements along the jet centerline are shown in Figure 6 for air injected

into both air and water. The decaying oscillatory pattern of the static pressure for injection into air is a result of a series of shock-cells which eventually erode due to the mixing layer encroachment toward the centerline. The pressure oscillations increase in magnitude and wavelength with increasing underexpansion ratio, as previously shown by Sheeran and Dosanjh[18]. The static pressure probe is expected to cause some smearing of the oblique and normal shock waves.

The most interesting result illustrated in Figure 6 is that the static pressure distribution in water is very similar to that for injection into air, at least for the first one or two shock-cells. This is clear evidence that a compressible wave field exists for underexpanded gas jets injected into a liquid, although the presence of the liquid clearly modifies the shock-cell structure. The main difference appears to be that more rapid mixing causes erosion of the external expansion field due to the multiphase interaction starting at an x/b of roughly four; this difference was substantiated by the shadowgraphs as well. This behavior is reasonable, since Chen and Faeth[5] show that turbulent mixing is invariably more rapid for injection of air into water than air into air.

The secondary shock-cell spacings are illustrated in Figure 7 for air injected into air and water based on the pressure distributions, as well as measurements obtained from shadowgraph images reported by Sheeran and Dosanjh[18] and Powell[22]. Present measurements of shock-cell spacing using a slot aspect ratio of eleven are in reasonable agreement with the spacing found by Sheeran and Dosanjh[18] using a slot aspect ratio of eight, but both these results differ from data obtained by Powell[22] where the aspect ratio was only 1.7, particularly at higher underexpansion ratios. The results obtained by Powell[22] probably have increased effects of sidewall shock-boundary-layer interaction, which was confirmed in this laboratory to reduce the expected shock-cell lengths. The shock cell lengths for air injected into water suggest the external expansion field is at least initially very similar to the case of air injected into air.

Measured and predicted lateral time-averaged void fraction profiles for the plane jets is plotted as a function of y/x in Figure 8 for an underexpansion ratio of two. The striking feature of the flow is the large lateral widths of the void fraction profiles, i.e. y/x of 0.5 for the near injector region which is two to three times larger than widths associated with single-phase scalar properties. This behavior is observed since the void fraction, α, is an extremely sensitive indicator of mixing for the large density ratios of the present flow, especially when the void fractions are low. For example, when $f<<\rho_e/\rho_\infty$, void fraction becomes

$$\alpha = f\,\rho_\infty / \rho_e\,, \qquad (2)$$

where ρ_e and ρ_∞ are the densites at the injector exit and of the ambient evironment, and where f is the mass based mixture fraction (where $f_e=1$ and $f_\infty=0$). Present test conditions involve $\rho_\infty/\rho_e \approx 800$; therefore, from equation (2), α is still significant even when f is much smaller than values normally associated with the edge of a single-phase jet. In view of this, it is not surprising that jet widths are unusually large when interpreted from void fraction measurements.

The profile shapes for this near-injector region are, in general, not self-similar: they exhibit the effects of the external expansion region as the underexpansion ratio increases and indicate a rather wide multiphase mixing layer which appears to have a self-similar profile. Predicted and measured jet widths show reasonable agreement for the range of underexpansion ratios; however, the shapes of the predicted profiles for standard initial conditions are far too blunt in the radial direction, particularly near the passage exit. Thus, this discrepancy suggests the inability of the analysis to handle very low mixture fractions, ca. 10^{-3}; and its inability to describe details of the external expansion region, as well as effects of global unsteadiness on the flow mixing properties near the jet exit. The predictions using a mixed initial condition show the same agreement with respect to general flow width as the standard initial conditions, but better agreement with measured profile shapes; thus predictions are sensitive to initial mixing conditions.

Present measurements and EEC predictions of characteristic flow widths, $2y_{0.5}$, (defined as twice the radius where $\bar{\alpha}/\bar{\alpha}_c$ equals one-half) are shown as a function of x/b in Figure 9. The unusually large flow width for gas injection into a liquid is again evident from the present measurements. The characteristic flow width increases at all axial stations as the underexpansion ratio increases. Predicted and measured jet widths show reasonable agreement for the low underexpansion ratios; however, discrepancies increase at higher underexpansion ratios. This behavior is probably due to the inability of the incompressible EEC model to locally describe the deflection of the liquid surface caused by variations in the external expansion region (see Figure 4C).

Measured entrainment coefficients for the plane jet, defined by equation (1), are plotted along with EEC predictions in Figure 10. Also shown on the plot is the empirical relation given by Schneider[23] for gas injection into a still gas. The entrainment coefficient decreases with increasing axial distance from the jet exit; this trend can be found from scaling laws for a fully-developed turbulent jet. Indeed, the empirical relation given by Schneider[23] for gas jets into a gaseous environment exhibits a similar trend. The comparison between measurements and predictions, given by the EEC model with standard initial conditions, as illustrated in Figure 10 is generally not very good. As before, the discrepancies are probably due to the model's inability to account for the unsteady features of the flow near the jet exit. The improved agreement seen for the predictions using the mixed initial conditions further emphasizes the sensitivity of the flow to initial conditions and near-injector disturbances. In addition, the improved agreement suggests that mixing is rapidly enhanced near the injector exit for all underexpansion ratios tested, probably as a result of the intrinsic unsteadiness of the release.

Conclusions

The major conclusions of the present study are as follows:

1.) Shock-wave-containing external expansion regions are present for injection of underexpanded plane air jets into water, similar to the well-known underexpansion region for air injected into air; however, the more rapid mixing rate for air jets in water causes the external expansion region to decay more rapidly than for air jets into air.

2.) Increasing underexpansion ratios tends to reduce effects of unsteadiness as represented by a reduction of the flow disturbance frequency and intensity, noted from high-speed motion pictures for plane injectors. The strong pressure fields associated with the external expansion region probably play a role in stabilizing these flows at large underexpansion ratios.

3.) Underexpanded air jets in liquids exhibit unusually large flow widths compared to typical single-phase jets; this behavior can be attributed to the strong sensitivity of void fraction to mixing levels. The thick multiphase mixing layer noted in the near injector region is thought to be a result of the innate observed unsteadiness of the flow field.

4.) In spite of the large density ratio and complex mixing characteristics of the present flows, use of the model based on locally-homogeneous flow and equivalent jet exit approximations yielded encouraging predictions of flow properties, although performance was sensitive to initial conditions. Deficiencies of the predictions are largely attributed to the global unsteadiness of the flow, since the LHF approximation tends to overestimate mixing for a steady flow.

Acknowledgements

The financial support of the Office of Naval Research (Contract No. N00014-85-0604) under technical management of G. D. Roy, R. S. Miller, and L. A. Parnell is gratefully acknowledged.

References

1. Cho, D. H., D. R. Armstrong and L. Bova (1987), "Dynamic Behavior of Reacting Gas Jets Submerged in Liquids: A Photographic Study," ONR Technical Report ANL-86-41.

2. Lin, M.-C. Jane (1986), "Transient Gas Jets in Liquids," Ph.D. Thesis, California Institute of Technology, Pasadena, CA.

3. Surin, V. A., V. N. Erchenko and V. M. Rubin (1983), "Propagation of a Gas Jet in a Liquid," *J. Engr. Phys.* **45**, pp. 1091-1101.

4. Kerney, P. J., G. M. Faeth, and D. R. Olson (1972), "Penetration Characteristics of a Submerged Steam Jet," *AIChE J.* **18**, pp. 548-553.

5. Chen, L. D. and G. M. Faeth (1983), "Structure of Turbulent Reacting Gas Jets in Submerged in Liquid Metals," *Combust. Sci. Tech.* **31**, pp. 277-296.

6. Avery, J. F. and G. M. Faeth (1975), "Combustion of a Submerged Gaseous Oxidizer Jet in a Liquid Metal," *Fifteenth Symposium (International) on Combustion*, The Combustion Institute, Pittsburgh, pp. 419-428.

7. Tross, S. R. (1974), "Characteristics of a Turbulent Two-Phase Submerged Free Jet," M. S.

Thesis, The Pennsylvania State University, University Park, PA.

8. Eggers, J. M. (1966), "Velocity Profiles and Eddy Viscosity Distributions Downstream of a Mach 2.2 Noxzzle Exhausting into Quiescent Air," NASA TN D-3601.

9. Ohba, K. (1979), "Relationship between Radiation Transmissivity and Void Fraction in Two-Phase Dispersed Flow," Tech. Rept. Osaka University 29, pp. 245-254.

10. Loth, E. (1988), "Underexpanded Air Jets in Water," Ph.D. Thesis, University of Michigan, Ann Arbor, MI.

11. Faeth, G. M. (1983), "Evaporation and Combustion of Sprays," *Prog. Energy Combust. Sci.* **9**, pp. 1-76.

12. Ruff, G. A., A. D. Sagar and G. M. Faeth (1988), "Structure and Mixing Properties of Pressure-Atomized Sprays, " *AIAA J.*, in press.

13. Sun, T. Y., R. N. Parthasarathy and G. M. Faeth (1986), "Bubbly Condensing Jets-- I. Methods and Near Source Properties; --II. Mean and Turbulent Structure," *J. of Heat Transfer* **108**, pp. 951-959.

14. Cheuch, S. G., M. C. Lai and G. M. Faeth (1988), "Structure of Turbulent Sonic Underexpanded Free Jets," *AIAA J.*, in press.

15. Bilger, R. W. (1976), "Turbulent Jet Diffusion Flames," *Prog. Energy Combust. Sci.* **1**, pp. 87-109.

16. Lai, M. C., S.-M. Jeng and G. M. Faeth (1986), "Structure of Turbulent Adiabatic Wall Plumes," *J. Heat Transfer* **108**, pp. 827-834.

17. Loth, E. and G. M. Faeth (1987), "Noncondensing Round Turbulent Gas Jets in Liquids," Interim Report, Navy Contract No. N00014-85-0604, Dept. of Aerospace Engineering, The University of Michigan, Ann Arbor, MI.

18. Sheeran, W. J. and D. S. Dosanjh (1966), "Investigations of Interacting Jet Flows -- Part II: A) Single, Two-Dimensional, Underexpanded Jet Flows From a Sonic Nozzle, B) Interaction of Transversely Impinging, Two-Dimensional Jet Flows," Rept. ME 1058-6608F, Syracuse University Research Institute, Depart. of Mechanical and Aerospace Engineering, Syracuse University, Syracuse NY.

19. Sherman, P. M., D. R. Glass and K. G. Duleep (1976), "Jet Flow Field During Screech," *Appl. Sci. Res.* **32**, pp. 283-303.

20. Glass, D. R. (1966), "The Effects of Acoustic Feedback on the Spread and Decay of Supersonic Jets," Aero. Engr. Thesis, The University of Michigan, Ann Arbor .

21. Borisov, A. A., B. E. Gelfand and E. I. Timofeev (1983), "Shock Waves in Liquids Containing Gas Bubbles," *Intl. J. Multiphase Flow* **9**, pp. 531-543.

22. Powell, A. (1953), "On the Noise Emanating from a Two-Dimensional Jet above the Critical Pressure," *Aero. Quart.* **4**, pp. 103-122.

23. Schneider, W. (1985), "Decay of Momentum Flux in Submerged Jets," *J. Fluid Mech.* **154**, pp. 91-110.

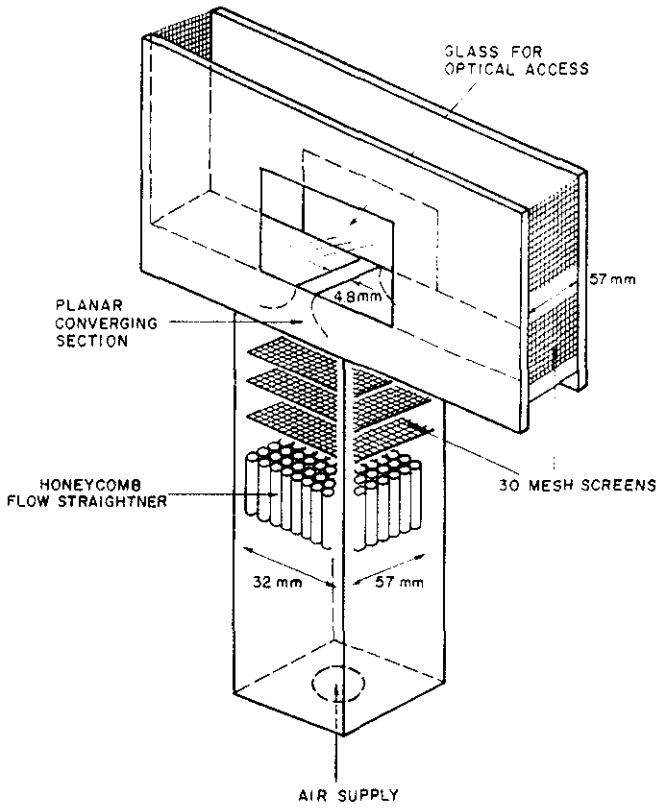

Figure 1. Sketch of plane injector assembly.

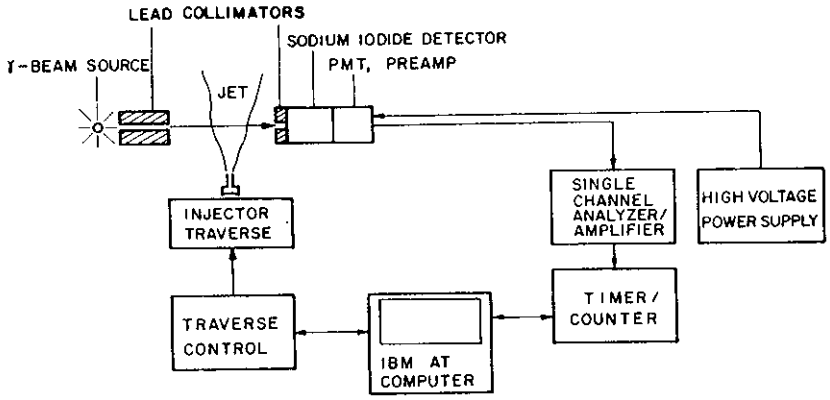

Figure 2. Sketch of gamma-ray absorption system.

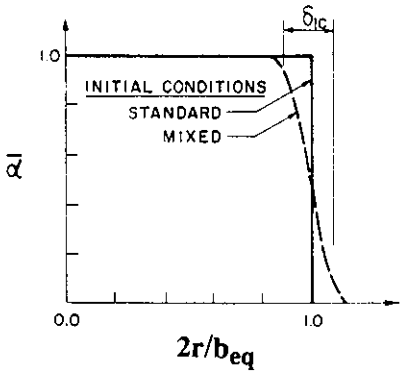

Figure 3. Initial conditions on α for EEC model.

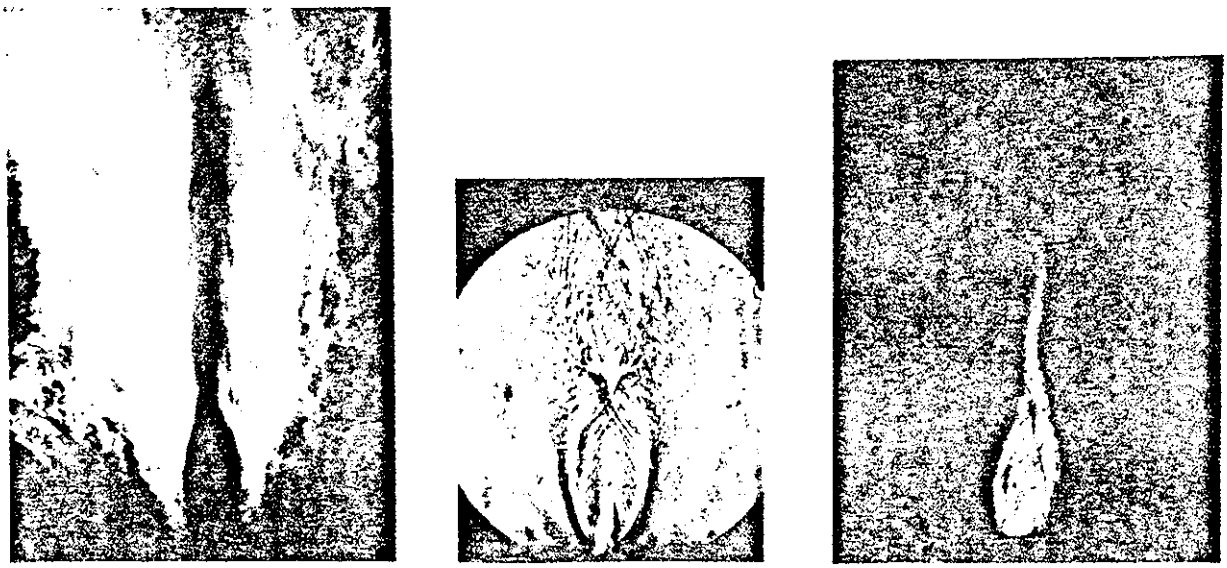

Figure 4. Underexpanded plane air jet at $\dot{m}/\dot{m}_S$=3.0:
A) flash photograph of air into water,
B) shadowgraph of air into air,
C) shadowgraph of air into water.

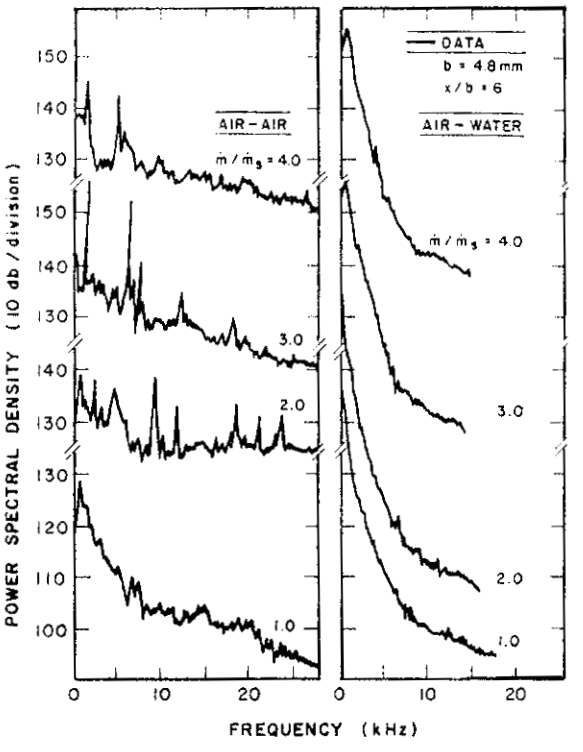

Figure 5. Power spectral density of acoustic signal.

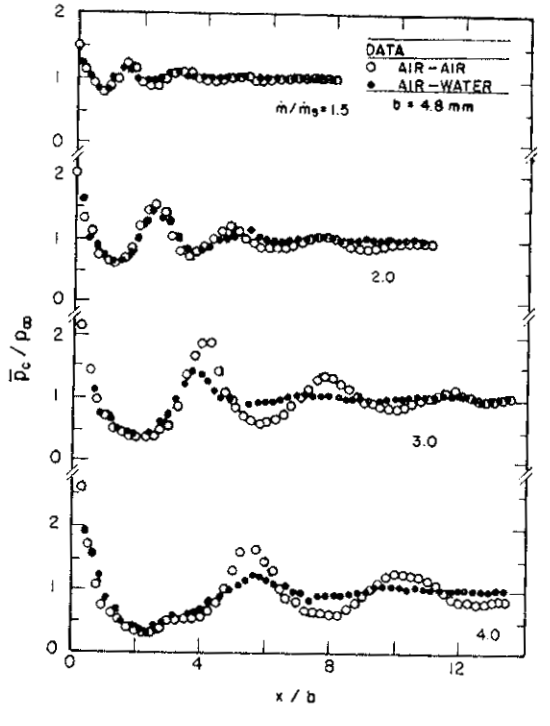

Figure 6. Centerline static pressure distribution.

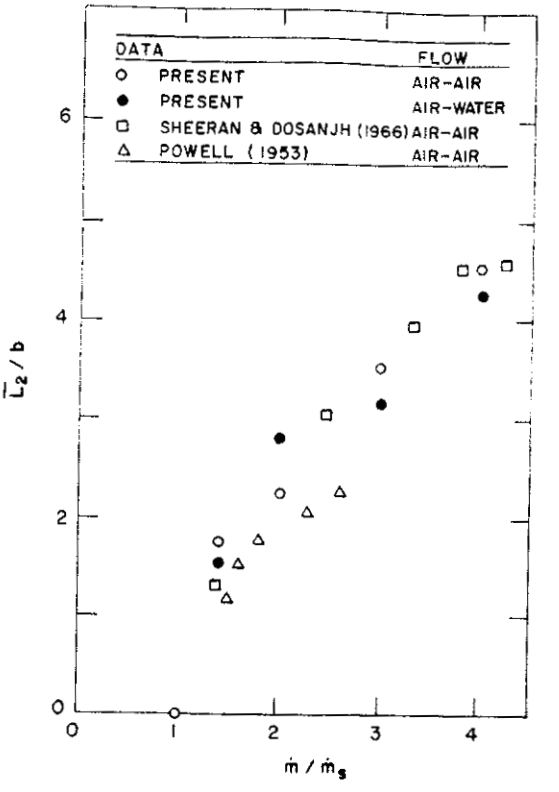

Figure 7. Shock-cell spacing for various underexpansion ratios.

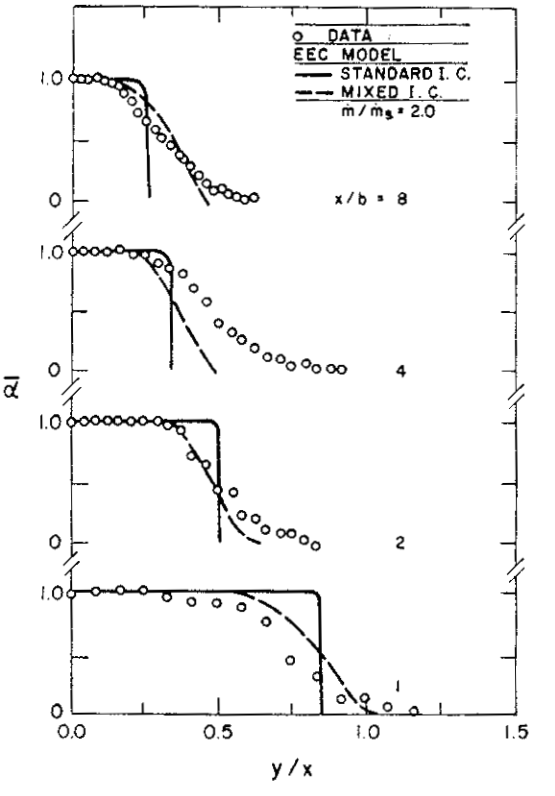

Figure 8. Lateral variation of mean void fraction at $\dot{m}/\dot{m}_S = 2.0$.

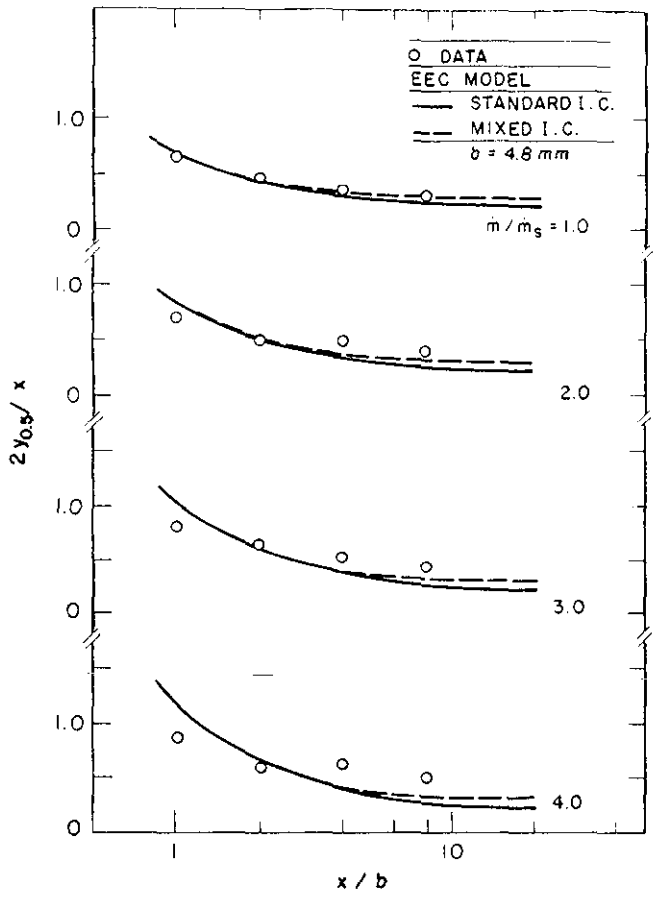

Figure 9. Axial variation of plane jet width, based on void fraction.

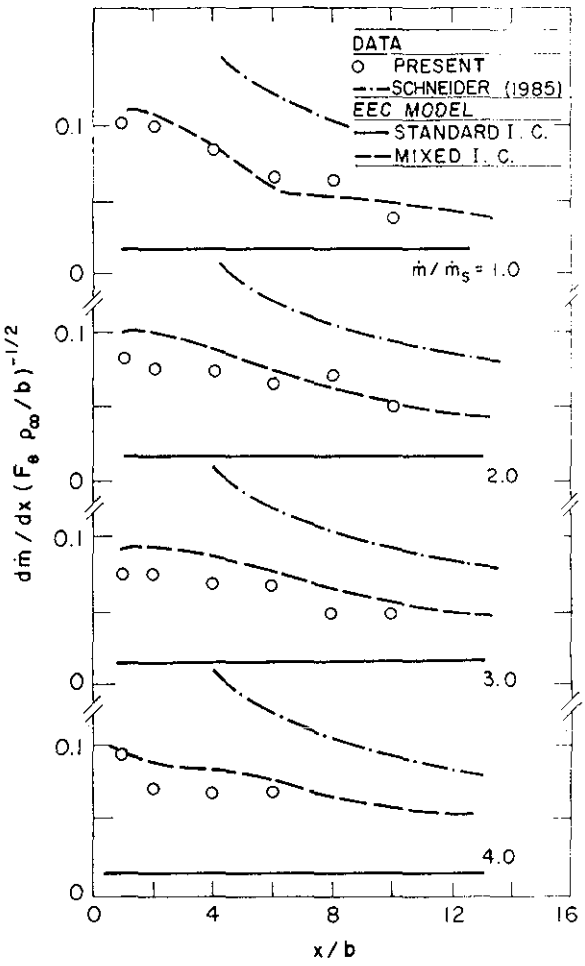

Figure 10. Axial variation of dimensionless entrainment coefficient.